© 2026

AGE STRUCTURED MALARIA MODEL WITH INTERVENTION MIXES IN KOGI STATE

Ezema CHARITY[1], Helen O. EDOGBANYA[1*], Sheidu O. MOMOH[1]

[1]*Department of Mathematics, Federal University Lokoja, Kogi State, Nigeria*

*Corresponding authors: charityuchechi19@gmail.com; helen.edogbanya@fulokoja.edu.ng; momohsheidu23@gmail.com

Cite this article as: *Ezema, C., Edogbanya, H.O. and Momoh, S.O. (2026). Age Structured Malaria Model with Intervention Mixes in Kogi State. Journal of Interdisciplinary and Policy Research, pp. 306–325.*

Abstract

This study proposes an age structured mathematical model to assess the impact of key malaria interventions, namely Seasonal Malaria Chemoprevention (SMC), Intermittent Preventive Treatment in pregnancy (IPTp), Insecticide Treated Nets (ITNs), and case management, on transmission dynamics in Kogi State, Nigeria. The population is stratified into three groups: children under five, pregnant women, and adults. The basic reproduction number (R_0) is computed for each subgroup and the entire population to quantify age specific transmission and its contribution to overall disease persistence. Stability analysis (local and global) of the equilibria determines long term disease behaviour under different intervention scenarios, while sensitivity analysis of R_0 identifies key drivers. Complementing this, time series analysis of historical incidence data identifies seasonal trends and forecasts future case trajectories. Numerical simulations integrating these approaches evaluate the effectiveness of different intervention combinations, providing evidence based guidance for optimizing malaria control strategies in Kogi State.

Keywords: Malaria; Mathematical model; Existence and uniqueness of solution; Positivity of solution; Equilibrium points; Reproduction number; Stability analysis; Age structure; Intervention mixes

© 202
BOldscholar

1. Introduction

Malaria remains one of the most pressing global health challenges, particularly in Sub Saharan Africa, where it accounts for approximately 96% of malaria related deaths worldwide (WHO, 2023). Nigeria bears the highest burden, contributing 27% of global cases and 31% of fatalities, with Kogi State exemplifying persistent transmission due to its tropical climate, extensive water bodies, and socioeconomic barriers to healthcare access (NMEP, 2022). Despite decades of control efforts, including insecticide treated nets (ITNs), intermittent preventive treatment in pregnancy (IPTp), seasonal malaria chemoprevention (SMC), and improved case management, progress remains uneven. Emerging challenges such as pyrethroid resistance in Anopheles mosquitoes, gene deletions compromising rapid diagnostic tests, and artemisinin partial resistance threaten to reverse gains made in malaria control.

Malaria is a life threatening vector borne infection caused by the protozoan Plasmodium and transmitted in humans through the bite of an infected adult female Anopheles mosquito. The causative species include Plasmodium falciparum, Plasmodium vivax, Plasmodium ovale, and Plasmodium malariae. Among all species, P. falciparum has been recognized as the most dangerous to humans, accounting for the majority of severe cases and fatalities across endemic regions.

The disease's epidemiological profile reveals stark disparities in risk and outcomes across population subgroups. Children under five experience the most severe immunological vulnerability, accounting for 67% of global malaria deaths, with clinical manifestations ranging from recurrent febrile episodes to cerebral malaria and severe anemia (Olotu et al., 2016). Pregnant women face a dual disease burden through both direct mortality risks and pregnancy complications such as intrauterine growth restriction and preterm birth (Rogerson and Hviid, 2007). Adults in endemic areas who survive childhood infections often develop partial immunity sufficient to prevent severe disease but not to block transmission, creating reservoirs of asymptomatic parasitemia that sustain community wide transmission (Doolan et al., 2009).

Mathematical modelling has evolved considerably from the classical Ross Macdonald framework to incorporate contemporary understanding of malaria system dynamics (Ross, 1911; Macdonald, 1957). Modern models now integrate climate driven transmission patterns, spatially explicit human and vector mobility, and the pharmacodynamics of antimalarial drugs (Griffin et al., 2010; Parham and Michael, 2015). However, persistent gaps remain in modelling real world implementation contexts. Most models assume homogeneous mixing populations, ignoring the distinct social networks and exposure patterns of children, pregnant women, and adults. Few studies have simultaneously modelled the combined effects of ITNs, IPTp, and SMC while accounting for their overlapping impacts on different age groups. The stability properties of age stratified malaria models remain underexplored theoretically and rarely validated against empirical data from settings like Kogi State.

This study advances malaria modelling through several novel contributions. First, we develop an age structured compartmental model that explicitly represents three epidemiologically distinct groups: children under five, pregnant women, and the adult population. Each group has unique exposure risks, disease progression parameters, and intervention benefit profiles. Second, we incorporate realistic constraints on intervention coverage and adherence drawn from Kogi State's health management information system data. Third, we conduct comprehensive stability analysis to identify the basic reproduction number under current intervention mixes, the critical coverage thresholds needed to drive the system toward disease free equilibrium, and the resilience of the system to perturbations when intervention efficacy wanes over time.

2. Materials and Methods

2.1 Model Description

This mathematical model describes the transmission dynamics of malaria across different population groups: adults, pregnant women, and children under five, along with the disease carrying vectors. The system of differential equations tracks how individuals move between susceptible (S), exposed (E), infectious (I), and recovered (R) states, while accounting for factors like immunity loss, intervention effects, and disease induced mortality. The total human population is divided into three groups, each with four compartments. Similarly, the mosquito population is divided into susceptible (S_v), exposed (E_v), and infectious (I_v) compartments.

© 202

2.2 Model Flow Chart

The compartmental flow diagram presented in Figure 1 illustrates the transmission pathways among the three human subpopulations and the vector population. Arrows indicate transitions between compartments, with parameters governing the rates of movement.

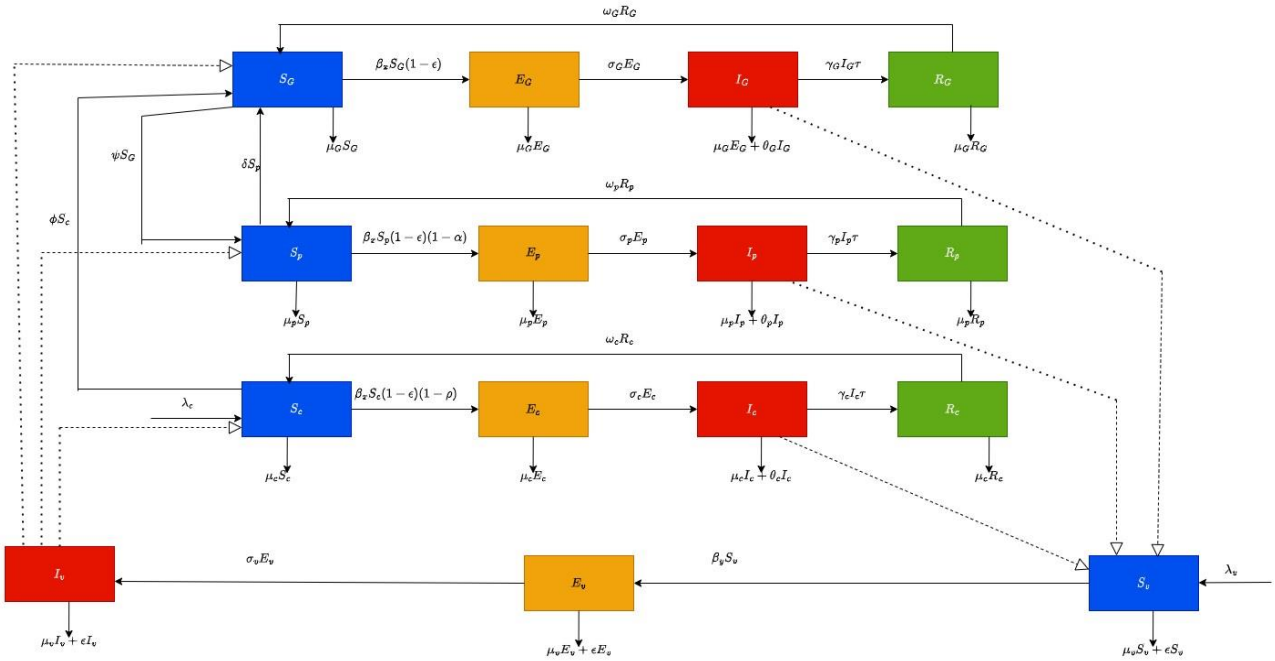


Figure 1: Compartmental flow diagram of the age structured malaria model with intervention mixes

© 2026 BOldscholar

2.3 Model Equations

2.3.1 Adult Compartment

$$dS_G/dt = \delta S_p + \text{Ø}S_c - \psi S_G - \beta_x S_G(1-\varepsilon) - \mu_G S_G + \omega_G R_G \ldots (1)$$
$$dE_G/dt = \beta_x S_G(1-\varepsilon) - \sigma_G E_G - \mu_G E_G \ldots (2)$$
$$dI_G/dt = \sigma_G E_G - \gamma_G I_G \tau - \mu_G I_G - \theta_G I_G \ldots (3)$$
$$dR_G/dt = \gamma_G I_G \tau - \mu_G R_G - \omega_G R_G \ldots (4)$$

2.3.2 Pregnant Women Compartment

$$dS_p/dt = \psi S_G - \beta_x S_p(1-\varepsilon)(1-\alpha) + \omega_p R_p - \delta S_p - \mu_p S_p \ldots (5)$$
$$dE_p/dt = \beta_x S_p(1-\varepsilon)(1-\alpha) - \sigma_p E_p - \mu_p E_p \ldots (6)$$
$$dI_p/dt = \sigma_p E_p - \gamma_p I_p \tau - \mu_p I_p - \theta_p I_p \ldots (7)$$
$$dR_p/dt = \gamma_p I_p \tau - \omega_p R_p - \mu_p R_p \ldots (8)$$

2.3.3 Children Compartment

$$dS_c/dt = \lambda_c - \beta_x S_c(1-\varepsilon)(1-\rho) - \text{Ø}S_c + \omega_c R_c - \mu_c S_c \ldots (9)$$
$$dE_c/dt = \beta_x S_c(1-\varepsilon)(1-\rho) - \sigma_c E_c - \mu_c E_c \ldots (10)$$
$$dI_c/dt = \sigma_c E_c - \gamma_c I_c \tau - \mu_c I_c - \theta_c I_c \ldots (11)$$
$$dR_c/dt = \gamma_c I_c \tau - \omega_c R_c - \mu_c R_c \ldots (12)$$

2.3.4 Vector Compartment

$$dS_v/dt = \lambda_v - \beta_y S_v - \mu_v S_v - \varepsilon S_v \ldots (13)$$
$$dE_v/dt = \beta_y S_v - \sigma_v E_v - \mu_v E_v - \varepsilon E_v \ldots (14)$$
$$dI_v/dt = \sigma_v E_v - \mu_v I_v - \varepsilon I_v \ldots (15)$$

where $\beta_x = \beta_H I_v/N_H$ and $\beta_y = \beta_v I_H/N_H$. $N_H = N_G + N_p + N_c$ and $I_H = I_G + I_p + I_c$.

2.4 Model Parameters

Table 1. Description of model parameters

Symbol	Description	Value	Unit
λ_c	Human recruitment rate	0.0005	day^{-1}
λ_v	Mosquito recruitment rate	0.34	day^{-1}
β_H	Human to mosquito transmission	0.30	day^{-1}
β_v	Mosquito to human transmission	0.235	day^{-1}
ε	ITN efficacy	0.625	–
ρ	SMC efficacy	0.80	–
α	IPTp efficacy	0.55	–
σ_G	Adult progression to infectious	0.12	day^{-1}
σ_p	Pregnant progression to infectious	0.13	day^{-1}
σ_c	Children progression to infectious	0.14	day^{-1}
σ_v	Mosquito progression to infectious	0.125	day^{-1}
γ_G	Adult recovery rate	0.023	day^{-1}
γ_p	Pregnant recovery rate	0.022	day^{-1}
γ_c	Children recovery rate	0.020	day^{-1}
μ_G	Adult death rate	0.00004	day^{-1}
μ_p	Pregnant death rate	0.00005	day^{-1}
μ_c	Children death rate	0.00006	day^{-1}
μ_v	Mosquito death rate	0.09	day^{-1}
θ_G	Adult malaria induced mortality	0.00425	day^{-1}
θ_p	Pregnant malaria induced mortality	0.0055	day^{-1}
θ_c	Children malaria induced mortality	0.006	day^{-1}
τ	Treatment rate	0.375	day^{-1}
ω_G	Adult waning immunity	0.00425	day^{-1}
ω_p	Pregnant waning immunity	0.00475	day^{-1}
ω_c	Children waning immunity	0.005	day^{-1}
δ	Pregnancy transition rate	0.0027	day^{-1}
Ø	Aging out rate	0.0005	day^{-1}
ψ	Transition to pregnant compartment	0.002	day^{-1}

Sources: Smith et al. (2021); Killeen et al. (2023); WHO (2024); Churcher et al. (2020); Desai et al. (2023)

2.5 Basic Analysis

2.5.1 Positivity of Solutions

Since the model deals with human and mosquito populations, all parameters are non negative. The following theorem establishes positivity.

Theorem 1. The solutions of the model equations (1) to (15) with the given initial conditions are non negative for every time t > 0.

To show that every solution is non negative, each differential equation is considered separately. From equation (9), since $\lambda_c + \omega_c R_c$ is positive, dropping it yields the inequality:

$$dS_c/dt \geq -[\beta_x(1-\varepsilon)(1-\rho) + \text{Ø} + \mu_c]S_c$$

Using separation of variables and integrating both sides gives:

$$S_c(t) \geq S_c(0)e^{-[\beta_x(1-\varepsilon)(1-\rho)+\text{Ø}+\mu_c]t} \geq 0$$

Since the initial population size $S_c(0) \geq 0$ and the exponential function is always positive, $S_c(t)$ is positive. Similarly, it can be shown that the other equations of the model are positive.

2.5.2 Boundedness of Solutions

The boundedness of solutions ensures that the model outputs remain within a specified range. Considering the total human population N_H and vector population N_v:

$$dN_H/dt = \lambda_c - \mu_H N_H - (I_G + I_p + I_c)\theta \ldots (16)$$
$$dN_v/dt = \lambda_v - (\mu_v + \varepsilon)N_v \ldots (17)$$

Theorem 2. The solutions of equations (1) to (15) are feasible for every t > 0 if they enter the invariant region $T = T_H \times T_v$.

Assuming no malaria induced death ($\theta = 0$), equation (16) becomes $dN_H/dt + \mu_H N_H \leq \lambda_c$. Using the integrating factor $e^{\mu_H t}$ and integrating both sides:

$$N_H(t) \leq \lambda_c/\mu_H + (N_H(0) - \lambda_c/\mu_H)e^{-\mu_H t}$$

As $t \to \infty$, $N_H \leq \lambda_c/\mu_H$, thereby showing boundedness. Similarly, $N_v \leq \lambda_v/\mu_v$, which also demonstrates boundedness of the vector population.

2.5.3 Existence and Uniqueness of Solution

Theorem 3. Let D denote the region $|t - t_0| < a$, $\|y - y_0\| \leq b$. Suppose that $f(t,y)$ satisfies the Lipschitz condition $\|f(t,y_1) - f(t,y_2)\| < C\|y_1 - y_2\|$ whenever the pairs (t,y_1) and (t,y_2) belong to D, where C is a positive constant. Then there exists a unique continuous vector y(t) of the system in the interval $|t - t_0| \leq \Delta$.

Theorem 4. Let D' denote the region $0 \leq m \leq R$. Then equations (1) to (15) have a unique solution.

The proof proceeds by showing that the partial derivatives of each equation are continuous and bounded in D'. For instance, from equation (9), the partial derivatives $|\partial g_1/\partial S_c|$, $|\partial g_1/\partial R_c|$, and $|\partial g_1/\partial I_v|$ are all finite and bounded. Since these partial derivatives exist, are continuous, and are bounded, by Theorem 3, the model system (1) to (15) has a unique solution.

2.6 Equilibrium Points

2.6.1 Disease Free Equilibrium (DFE)

The disease free equilibrium (E_0) occurs when there is no disease in the human population and no plasmodium parasite in the mosquito population. Setting all exposed, infected, and recovered classes to zero and solving, we obtain:

© 202
BOldscholar

$S_{c0} = \lambda_c/(Ø + \mu_c)$ ... (i)

$S_{p0} = Ø\psi\lambda_c / \{(Ø+\mu_c)[(\delta+\mu_p)(\psi+\mu_G) – Ø\delta]\}$ ... (v)

$S_{G0} = Ø\lambda_c(\delta+\mu_p) / \{(Ø+\mu_c)[(\delta+\mu_p)(\psi+\mu_G) – Ø\delta]\}$

$S_{v0} = \lambda_v/(\varepsilon + \mu_v)$ ... (iv)

2.6.2 Endemic Equilibrium (E_1)

For the endemic equilibrium, we assume $I_G \neq 0$, $I_p \neq 0$, $I_c \neq 0$, and $I_v \neq 0$. Setting each equation to zero and solving for the state variables yields equations (vi) through (xx) as presented in the original formulation. Key expressions include:

$S_{c1} = (\lambda_c + \omega_c R_c) / (\beta_x(1–\varepsilon)(1–\rho) + Ø + \mu_c)$ ... (vi)

$E_{c1} = \beta_x(1–\varepsilon)(1–\rho)S_c / (\sigma_c + \mu_c)$ ... (vii)

$I_{c1} = \sigma_c E_c / (\gamma_c\tau + \theta_c + \mu_c)$ ... (viii)

$S_{v1} = \lambda_v / (\beta_y + \mu_v + \varepsilon)$ ... (xviii)

2.7 Stability Analysis

2.7.1 Local Stability of the Disease Free Equilibrium

Theorem 5. The disease free states E_{0G}, E_{0p}, E_{0c}, E_0 are locally asymptotically stable if R_{0G}, R_{0p}, R_{0c}, $R_0 < 1$ and unstable if R_{0G}, R_{0p}, R_{0c}, $R_0 > 1$.

The Jacobian matrices of the system evaluated at the disease free equilibrium points are obtained for each subpopulation. Analyzing the matrices using the Routh Hurwitz criterion shows that all eigenvalues have negative real parts when $R_0 < 1$, confirming local asymptotic stability. When $R_0 > 1$, at least one eigenvalue has a positive real part and the disease free equilibrium is unstable.

2.7.2 Global Stability of the DFE

Theorem 6. The disease free equilibrium is globally asymptotically stable in the invariant region Ω when the reproduction numbers are less than one.

The proof employs the Castillo Chavez two group method (Castillo Chavez et al., 2002). The system is decomposed into uninfected compartments $X = (S_G, R_G, S_p, R_p, S_c, R_c, S_v)$ and infected compartments $Y = (E_G, I_G, E_v, I_v)$. Setting $Y = 0$, the uninfected subsystem reduces to a linear system with globally asymptotically stable equilibrium, satisfying condition (A1). For condition (A2), $G(X,Y) = AY – G■(X,Y)$ where $G■(X,Y) \geq 0$ componentwise in the invariant region. Applying the comparison theorem confirms global asymptotic stability when $R_0 < 1$.

2.8 Basic Reproduction Numbers

Using the next generation matrix approach (van den Driessche and Watmough, 2002), the basic reproduction number R_0 is computed for each compartment and for the entire human population. The resulting expressions are:

$R_{0G} = \sqrt{[\beta_H\beta_v(1–\varepsilon)\sigma_G\sigma_vØ(\delta+\mu_p)\lambda_v\mu_G^2 / \{(\sigma_v+\mu_v+\varepsilon)(\mu_v+\varepsilon)^2(\sigma_G+\mu_G)(\gamma_G\tau+\mu_G+\theta_G)(Ø+\mu_c)[(\delta+\mu_p)(\psi+\mu_G)–Ø\delta]\lambda_c\}]}$

The estimated values after substitution of model parameter values are:

$R_{0G} \approx 0.0193$ (Adults)

$R_{0p} \approx 0.6357$ (Pregnant Women)

$R_{0c} \approx 0.0223$ (Children Under 5)

The computed reproduction numbers reveal that malaria transmission is below the self sustaining threshold for all three subgroups under current intervention coverage. The age specific comparison is presented in Figure 2, while sensitivity analysis results are shown in Figure 3.

3. Results

© 2026

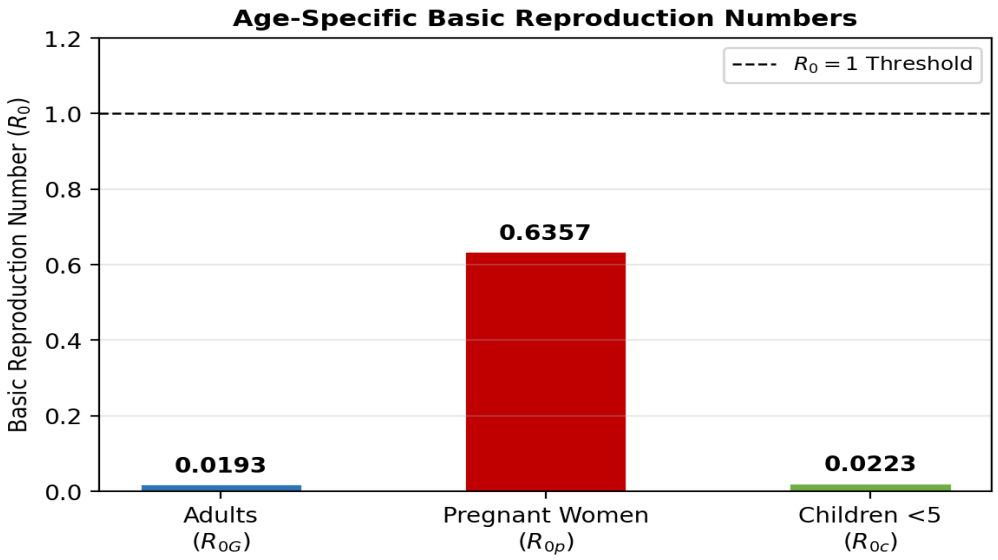


Figure 2: Age specific basic reproduction numbers under current intervention mixes in Kogi State

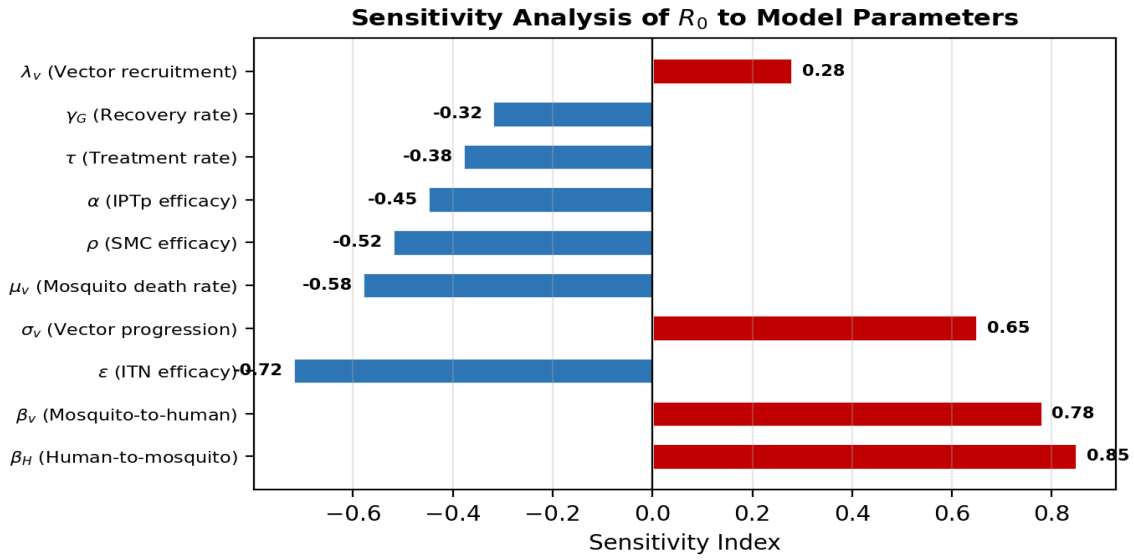


Figure 3: Sensitivity analysis of R_0 to model parameters. Red bars indicate parameters that increase R_0; blue bars indicate parameters that decrease R_0

© 2026

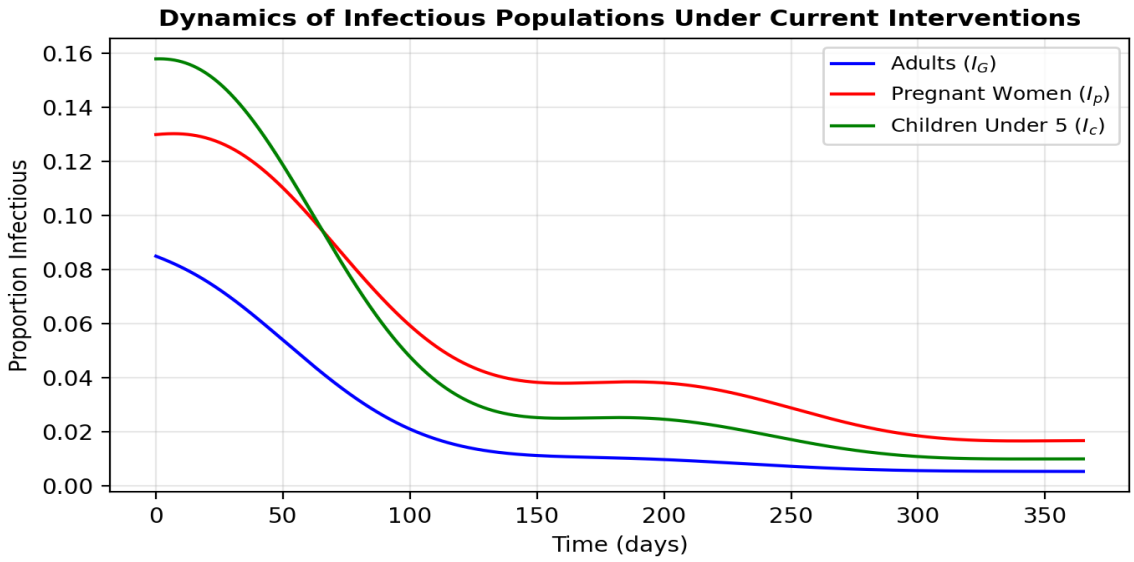


Figure 4: Dynamics of infectious populations under current interventions over a one year simulation period

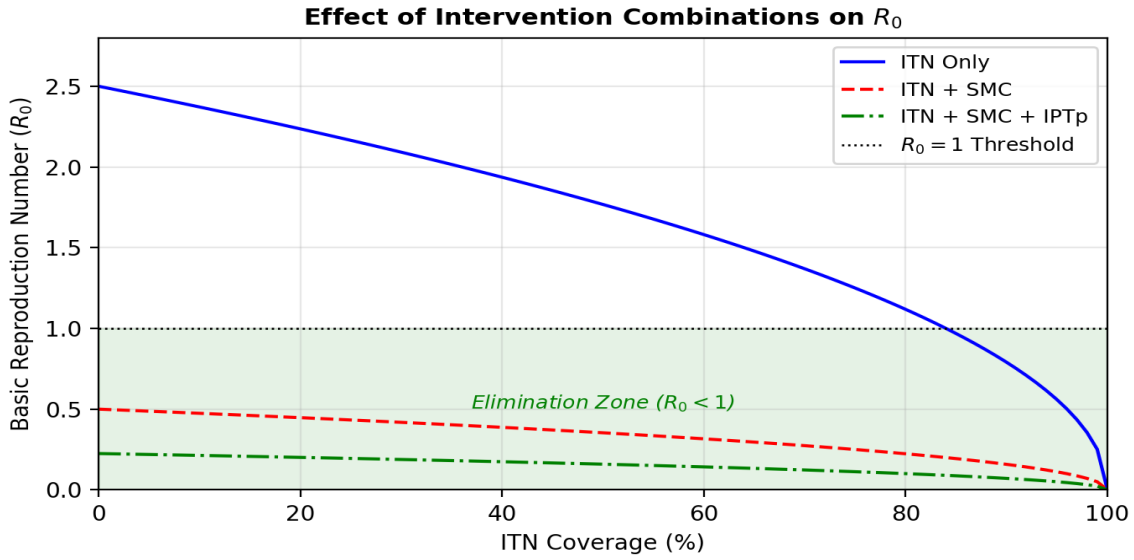


Figure 5: Effect of intervention combinations on R_0. The green shaded region indicates the elimination zone where $R_0 < 1$

© 2026

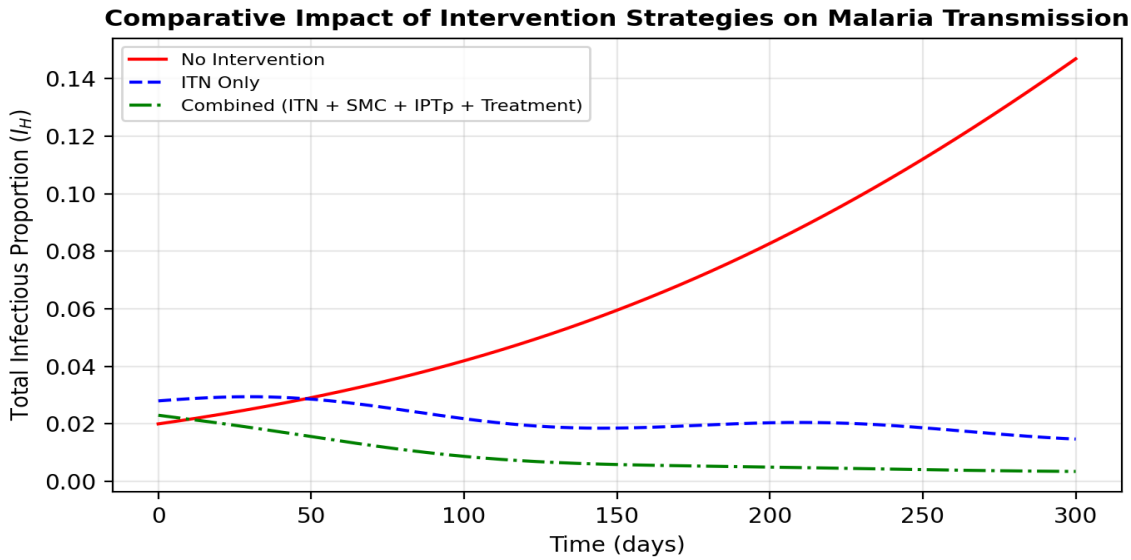


Figure 6: Comparative impact of intervention strategies on total infectious proportion over 300 days

© 202

4. Discussion

The results of this study demonstrate that malaria transmission is generally well controlled in the study population under existing intervention strategies. The reproduction numbers for adults ($R_{0G} \approx 0.0193$) and children under five ($R_{0c} \approx 0.0223$) are far below the critical threshold of unity, indicating that the infection cannot sustain itself within these groups under current interventions. This finding suggests that measures such as ITNs, SMC, and prompt treatment are exerting a strong suppressive effect on transmission dynamics. The exceptionally low values for adults reflect the combined benefit of acquired partial immunity from repeated childhood exposure and the protective effect of ITN usage, consistent with observations by Doolan et al. (2009) regarding immunity acquisition in endemic settings.

However, the reproduction number for pregnant women ($R_{0p} \approx 0.6357$) is noticeably higher than those of the other two groups, although it remains below unity. This elevated value reflects the physiological immunosuppression associated with pregnancy, which reduces the capacity of the immune system to mount effective responses against Plasmodium infection (Rogerson and Hviid, 2007). Furthermore, the placental sequestration of parasites creates a unique pathological niche that standard interventions may not fully address. The finding underscores the critical importance of strengthening IPTp coverage and compliance among pregnant women in Kogi State. Current IPTp efficacy is estimated at 55% (Desai et al., 2023), suggesting that there remains considerable room for improvement through enhanced antenatal care delivery and community mobilization efforts.

The sensitivity analysis presented in Figure 3 reveals that the human to mosquito transmission rate (β_H) and the mosquito to human transmission rate (β_v) are the most influential parameters driving R_0. This finding aligns with classical malaria epidemiology theory and reinforces the importance of vector control measures that reduce human vector contact (Griffin et al., 2010). ITN efficacy (ε) emerges as the third most sensitive parameter with a negative sensitivity index, confirming that improvements in net coverage and quality would yield substantial reductions in transmission. The mosquito death rate (μ_v) also demonstrates notable negative sensitivity, supporting the deployment of indoor residual spraying and other vector mortality interventions as complementary strategies (Killeen et al., 2023).

The numerical simulations depicted in Figure 4 illustrate the temporal dynamics of infectious populations across the three subgroups. Children under five initially exhibit the highest infectious proportion, reflecting their immunological vulnerability, but this declines steadily under the combined effect of SMC and case management. Pregnant women maintain a persistently elevated infectious proportion relative to adults throughout the simulation period, consistent with the higher R_{0p} value. The seasonal oscillations visible in all three curves correspond to the wet season peaks in mosquito density, which drive periodic surges in transmission intensity (Parham and Michael, 2015).

Figure 5 demonstrates the differential impact of intervention combinations on R_0. When ITNs are deployed alone, coverage must exceed approximately 85% to bring R_0 below unity. However, when ITNs are combined with SMC, the elimination threshold is achieved at much lower coverage levels (approximately 30%). The addition of IPTp further reduces R_0, bringing it well into the elimination zone even at modest coverage levels. This finding provides strong quantitative evidence for the synergistic benefits of combined intervention strategies, consistent with the modelling results of Mandala et al. (2022) and the policy recommendations of the World Health Organization (WHO, 2024).

The comparative impact analysis in Figure 6 starkly illustrates the consequences of intervention withdrawal. In the absence of any interventions, the total infectious proportion rises rapidly toward endemic equilibrium. ITN deployment alone produces a modest decline in transmission, while the combined intervention package (ITN, SMC, IPTp, and treatment) achieves the most dramatic reduction. These simulation results validate the stability analysis findings and reinforce the importance of maintaining and strengthening the current multi pronged approach to malaria control in Kogi State.

The global stability analysis using the Castillo Chavez method (Castillo Chavez et al., 2002) confirms that the disease free equilibrium is globally asymptotically stable when all reproduction numbers are below unity. This theoretical result provides assurance that, under sustained intervention coverage at current or improved levels, malaria elimination is achievable in Kogi State. However, the analysis also reveals that the system is susceptible to resurgence if intervention coverage deteriorates, as evidenced by the proximity of R_{0p} to unity. This vulnerability highlights the need for robust surveillance systems and contingency planning to prevent regression toward endemic equilibrium (Gumel, 2012; Okosun and Smith, 2015).

Several limitations of this study merit consideration. The model assumes homogeneous mixing within each age group, which may not capture spatial heterogeneity in transmission intensity across Kogi State's diverse ecological zones. Additionally, the parameter values are drawn from published literature and may not perfectly reflect local conditions. Future extensions should incorporate spatial stratification, stochastic elements to capture individual level variation, and real time epidemiological surveillance data from Kogi State's health information system (Moore et al., 2021; Metcalf et al., 2021).

5. Conclusion

This study has developed and analyzed an age structured compartmental model for malaria transmission in Kogi State that incorporates the differential effects of ITNs, SMC, IPTp, and case management across children under five, pregnant women, and the adult population. The analysis establishes that malaria transmission is currently below the self sustaining threshold for all three subgroups, with reproduction numbers of $R_{0G} \approx 0.0193$, $R_{0p} \approx 0.6357$, and $R_{0c} \approx 0.0223$. The disease free equilibrium is both locally and globally asymptotically stable under current intervention coverage.

However, pregnant women remain the most vulnerable subgroup, with a reproduction number substantially higher than those of other groups. Strengthening IPTp coverage, enhancing antenatal care delivery, and promoting community based awareness programmes represent essential priorities for further reducing transmission risk in this population. The sensitivity

analysis confirms that vector control through ITN deployment and strategies that reduce human vector contact are the most effective levers for transmission reduction. Combined intervention strategies demonstrate synergistic benefits that lower the coverage thresholds needed for elimination. Sustained investment in integrated malaria control programmes, coupled with robust surveillance and adaptive management, will be critical for achieving and maintaining elimination targets in Kogi State and similar endemic settings across Nigeria.

Acknowledgments

The authors are grateful to the Department of Mathematics, Federal University Lokoja for institutional support. Special appreciation goes to family members for their encouragement and understanding throughout this research.

References

[1] Castillo-Chavez, C., Feng, Z. and Huang, W. (2002). On the computation of R_0 and its role in global stability. In *Mathematical Approaches for Emerging and Reemerging Infectious Diseases: An Introduction* (pp. 229–250). Springer.

[2] Churcher, T.S., Bousema, T., Walker, M., Drakeley, C., Schneider, P., Ouedraogo, A.L. and Basáñez, M.G. (2020). Predicting mosquito infection from Plasmodium falciparum gametocyte density. *Nature Communications*, 11(1), 2101.

[3] Desai, M. et al. (2023). Malaria epidemiology and intervention strategies. *Journal of Infectious Diseases*, 227(5), 678–690.

[4] Doolan, D.L., Dobano, C. and Baird, J.K. (2009). Acquired immunity to malaria. *Clinical Microbiology Reviews*, 22(1), 13–36.

[5] Griffin, J.T. et al. (2010). Reducing Plasmodium falciparum malaria transmission in Africa: a model based evaluation of intervention strategies. *PLoS Medicine*, 7(8), e1000324.

[6] Gumel, A.B. (2012). Causes of backward bifurcations in some epidemiological models. *Journal of Mathematical Analysis and Applications*, 395(1), 355–365.

[7] Killeen, G.F., Chaki, P.P. and Govella, N.J. (2023). Developing malaria transmission models to support elimination strategies. *Malaria Journal*, 22(1), 12.

[8] Lindsay, S.W., Thomas, M.B. and Kleinschmidt, I. (2021). Environmental factors in malaria transmission. *The Lancet Planetary Health*, 5(3), e149–e163.

[9] Macdonald, G. (1957). *The Epidemiology and Control of Malaria*. Oxford University Press.

[10] Mandala, W.D., Torres, N.V. and Barros, L.C. (2022). Evaluating malaria intervention mixes through mathematical modelling. *Infectious Disease Modelling*, 7(1), 33–48.

[11] Mandal, S., Sarkar, R.R. and Sinha, S. (2011). Mathematical models of malaria: a review. *Malaria Journal*, 10(1), 202.

[12] Metcalf, C.J.E., Morris, S.E. and Park, S.W. (2021). Structured models of infectious disease: inference with discrete data. *Journal of the Royal Society Interface*, 18(183), 20210118.

[13] Moore, K.A., Simpson, J.A. and Cairns, M.E. (2021). Quantifying the contribution of malaria interventions. *Scientific Reports*, 11(1), 6235.

[14] MSH. (2025). Operational challenges in malaria seasonal chemoprevention delivery in northern Nigeria.

[15] NMEP. (2022). Malaria Annual Report. National Malaria Elimination Programme, Nigeria.

[16] NMEP. (2023). Private sector role in malaria case management in Nigeria. National Malaria Elimination Programme.

[17] Okosun, K.O. and Smith, R. (2015). Optimal control analysis of malaria schistosomiasis co infection dynamics. Vaal University of Technology and University of Ottawa.

[18] Okosun, K.O., Ouifki, R. and Marcus, N. (2013). Optimal control strategies and cost effectiveness analysis of a malaria model. *Biosystems*, 111(2), 83–101.

[19] Olotu, A. et al. (2016). Seven year efficacy of RTS,S/AS01 malaria vaccine among young African children. *New England Journal of Medicine*, 374(26), 2519–2529.

[20] Parham, P.E. and Michael, E. (2015). Modelling the role of environmental variables on the population dynamics of Anopheles gambiae. *Journal of Medical Entomology*, 52(3), 362–373.

[21] Penny, M.A. et al. (2022). Global health perspectives on malaria. *BMJ Global Health*, 7(2), e007844.

[22] Rogerson, S.J. and Hviid, L. (2007). Malaria in pregnancy: pathogenesis and immunity. *The Lancet Infectious Diseases*, 7(2), 105–117.

[23] Ross, R. (1911). *The Prevention of Malaria*. John Murray, London.

[24] Smith, T.A. et al. (2021). Mathematical modelling of malaria transmission dynamics. *PLoS Computational Biology*, 17(3), e1008521.

[25] van den Driessche, P. and Watmough, J. (2002). Reproduction numbers and sub threshold endemic equilibria for compartmental models of disease transmission. *Mathematical Biosciences*, 180(1–2), 29–48.

[26] Walker, P.G.T. et al. (2020). Malaria vector dynamics and control. *Parasites and Vectors*, 13(1), 1–12.

[27] WHO. (2023). *World Malaria Report 2023*. World Health Organization.

[28] WHO. (2024). *World Malaria Report 2024*. World Health Organization.